*sustainability*

MDPI

*Article*

# Spatiotemporal Distribution of $PM_{2.5}$ and $O_3$ and Their Interaction During the Summer and Winter Seasons in Beijing, China

**Hui Zhao [1], Youfei Zheng [1,2,*] and Chen Li [2]**

[1] Key Laboratory for Aerosol-Cloud-Precipitation of China Meteorological Administration, Nanjing University of Information Science and Technology, Nanjing 210044, China; zhaohui_nuist@163.com

[2] Key Laboratory of Atmospheric Environment Monitoring and Pollution Control, Collaborative Innovation Center of Atmospheric Environment and Equipment Technology, Nanjing University of Information Science and Technology, Nanjing 210044, China; papertg2018@163.com

* Correspondence: zhengyf@nuist.edu.cn

Received: 26 September 2018; Accepted: 27 November 2018; Published: 30 November 2018


**Abstract:** This study analyzed the spatiotemporal variations in $PM_{2.5}$ and $O_3$, and explored their interaction in the summer and winter seasons in Beijing. To this aim, hourly $PM_{2.5}$ and $O_3$ data for 35 air quality monitoring sites were analyzed during the summer and winter of 2016. Results suggested that the highest $PM_{2.5}$ concentration and the lowest $O_3$ concentration were observed at traffic monitoring sites during the two seasons. A statistically significant ($p < 0.05$) different diurnal variation of $PM_{2.5}$ was observed between the summer and winter seasons, with higher concentrations during daytime summer and nighttime winter. Diurnal variations of $O_3$ concentrations during the two seasons showed a single peak, occurring at 16:00 and 15:00 in summer and winter, respectively. $PM_{2.5}$ presented a spatial pattern with higher concentrations in southern Beijing than in northern areas, particularly evident during wintertime. On the contrary, $O_3$ concentrations presented a decreasing spatial trend from the north to the south, particularly evident during summer. In addition, we found that $PM_{2.5}$ concentrations were positively correlated ($p < 0.01$, $r = 0.57$) with $O_3$ concentrations in summer, but negatively correlated ($p < 0.01$, $r = -0.72$) with $O_3$ concentrations in winter.

**Keywords:** atmospheric pollution; particulate matter; $PM_{2.5}$; Ozone

## 1. Introduction

In recent years, serious air pollution has become one of the most important environmental problems along with the development of society and economy, especially in economically developed cities, such as Beijing, Shanghai, Guangzhou, and other big cities [1]. The major pollutants include particulate matter (e.g., $PM_{2.5}$ and $PM_{10}$), ground-level ozone ($O_3$), nitrogen oxides (NOx), sulfur dioxide ($SO_2$), carbon monoxide (CO), and Volatile Organic Compounds (VOCs) [2,3]. Many studies have suggested that high levels of air pollutants can cause some adverse effects [4–11]. The Chinese government has been dedicated to air pollution monitoring and control over last couple of decades, and ambient air quality has been widely measured in big cities since 1980s. In February 1988, the air pollution index (API), based on the concentrations of three atmospheric pollutants, namely total suspended particles (TSP), sulfur dioxide ($SO_2$), and nitrogen dioxide ($NO_2$), was introduced to assess the status of ambient air quality in China. On 5 June 2000, the China National Environmental Monitoring Center began to report API, defined according to the National Ambient Air Quality Standard (NAAQS-China, GB3095-1996) [12], by considering particulate matter ($PM_{10}$), sulfur dioxide ($SO_2$), and nitrogen dioxide ($NO_2$). From 18 January 2013, the Beijing municipal government has

promulgated the new National Ambient Air Quality Standards (NAAQS-China, GB3095-2012) [13], and publicized real time monitoring data of Air Quality Index (AQI) and six major atmospheric pollutants ($PM_{2.5}$, $O_3$, $PM_{10}$, CO, $NO_2$, and $SO_2$).

In particular, regional complex atmospheric pollution characterized by high levels of $O_3$ and $PM_{2.5}$ has become a major challenge in China [14,15]. $O_3$ is regarded as a secondary pollutant, primarily produced through a series of complex chemical reactions between Volatile Organic Compounds (VOCs) and nitrogen oxides ($NO_X$) under solar radiation in the wavelength range of 200 to 300 nm [16,17]. The formation of $O_3$ is a very complicated process which is affected by many factors, including precursor emissions (e.g., $NO_X$, CO, and VOCs), local climate conditions (e.g., temperature, relative humidity, solar radiation, and wind direction and speed), and atmospheric chemical processes [18–21]. Fine particulate matter with an aerodynamic diameter of less than 2.5 μm ($PM_{2.5}$) can scatter and/or absorb solar radiation and influence the surface radiation budget [22], and these scattering and/or absorbing properties are inherently related to its chemical composition. The carbonaceous components (e.g., OC and EC) and water-soluble ions (e.g., $SO_4^{2-}$, $NO_3^-$, and $NH_4^+$) are important chemical constituents of particulate matter [23,24]. In general, $PM_{2.5}$ in urban areas originates mainly from emission sources such as biomass burning, traffic-related emissions, road dust, and industrial and agricultural production as well as regional transported aerosols [25,26], while the remaining portions originate from natural sources [27]. To reduce emissions of air pollutants and improve air quality in China, the "Air Pollution Prevention and Control Action Plan" was formulated and released by the Chinese government on September 10, 2013. A recent study reported that its implementation has favored the reduction of air pollutants ($PM_{2.5}$, $PM_{10}$, $SO_2$, and $NO_X$) [28], but $O_3$ concentration showed an increasing trend from 2013 to 2017 [29–31]. Meanwhile, other studies also suggested that the implementation of air pollution control measures during some international events such as the APEC Meeting, the G20 summit, and some political events can result in the reduction in concentration of $PM_{2.5}$, while $O_3$ concentration increased [32,33]. As a result, it has been suggested that $PM_{2.5}$ and $O_3$ pollution and their interaction should be further investigated [34–36].

In fact, although many studies have reported on $PM_{2.5}$ and $O_3$ pollution, most of them focused on spatiotemporal distribution and their relationships with weather conditions; research on the interaction of $PM_{2.5}$ and $O_3$ in the atmosphere is still rare. Feng et al. [37] pointed out that high aerosol concentrations can significantly decrease photolysis frequencies and reduce $O_3$ concentration by more than 50 $\mu g/m^3$ in the summertime. In addition, previous studies also reported a significant positive correlation between $PM_{2.5}$ and $O_3$ concentrations during the summertime [38,39]. The discrepancy in these studies suggests that the interaction between $O_3$ and $PM_{2.5}$ in the atmosphere may vary over time across space, which should be further investigated.

In this paper, we analyzed hourly $PM_{2.5}$ and $O_3$ data collected at 35 air monitoring sites in Beijing during the summer (June–August 2016) and winter (December 2016–February 2017) seasons. Our primary objectives are thus to (i) analyze the spatiotemporal distribution of $PM_{2.5}$ and $O_3$ in Beijing and (ii) explore the interaction of $O_3$ and $PM_{2.5}$ in the atmosphere during the summer and winter seasons.

## 2. Methods

### *2.1. Study Area*

Beijing, situated in the north of China, is the capital city of China. It covers a total area of about 16,800 square kilometers with a population of more than 20 million. The city is constituted of 16 administrative subdivisions including a total of 14 urban and suburban districts and two rural counties. The vegetation coverage is mainly distributed in Northern Beijing, including Changping, Yanqing, Huairou, Miyun, and Pinggu Districts. Southern Beijing presents lower vegetation coverage due to the influence of urbanization. Beijing has experienced continuous economic growth and rapid urbanization over the past several decades. However, the rapid development of the economy has

generated a general decline in environmental quality; Beijing is currently considered as one of the cities with the most severe air pollution in China, and even globally [40].

### 2.2. Data Sources

In this study, $PM_{2.5}$ and $O_3$ hourly concentration data for Beijing were collected from a web platform (http://zx.bjmemc.com.cn/) made available from by Beijing Municipal Environmental Protection together with other air pollutants ($PM_{10}$, $SO_2$, $NO_2$, CO) for 35 air monitoring sites (Figure 1) since 2013 [15].

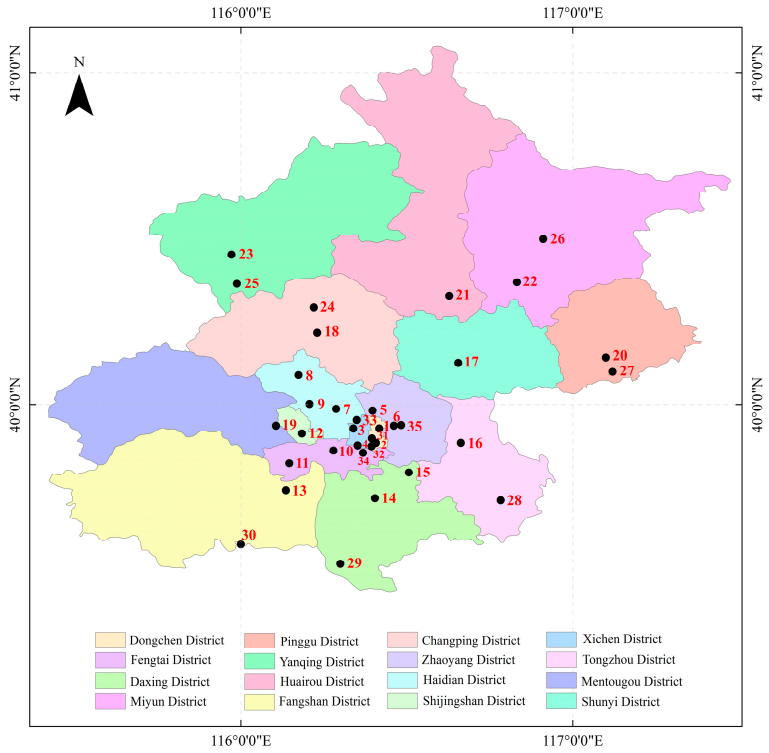


**Figure 1.** Locations of 35 ambient air quality monitoring sites in Beijing.

We divided the 35 air monitoring sites into four categories according to their functions (Table 1) [41]. In particular, hourly $PM_{2.5}$ and $O_3$ concentrations were obtained for summer 2016 (June–August 2016) and winter 2016/2017 (December 2016–February 2017).

**Table 1.** Category of each monitoring site in Beijing city.

| Site name | Category | Region | Code |
|---|---|---|---|
| Dongsi | Urban Sites (To assess air quality and its overall variation in the urban environment) | Center | 1 |
| Temple of Heaven | | Center | 2 |
| West Park Officials | | Center | 3 |
| West Wanshou Nishinomiya | | Center | 4 |
| Olympic Sports Center | | Center | 5 |
| Agricultural Exhibition Hall | | Center | 6 |
| Wanliu | | Center | 7 |
| Northern New Area | | Center | 8 |
| Botanical Garden | | Center | 9 |
| Fengtai Garden | | Center | 10 |
| Yungang | | Center | 11 |
| Shijingshan city | | Center | 12 |

**Table 1.** *Cont.*

| Site name | Category | Region | Code |
|---|---|---|---|
| Liangxiang | Suburban Sites (to characterize the variation of suburban air quality) | Southwest | 13 |
| Daxing | | Southeast | 14 |
| Yizhuang | | Southeast | 15 |
| Tongzhou | | Southeast | 16 |
| Shunyi | | Northeast | 17 |
| Changping | | Northwest | 18 |
| Mentougou | | Southwest | 19 |
| Pinggu | | Northeast | 20 |
| Huairou | | Northeast | 21 |
| Miyun | | Northeast | 22 |
| Yanqing | | Northwest | 23 |
| Dingling | Background Sites (to describe regional background levels and reflect the transmission of pollutants between regions) | Northwest | 24 |
| Badaling | | Northwest | 25 |
| Miyun Reservoir | | Northeast | 26 |
| Donggaocun | | Northeast | 27 |
| Yongledian | | Southeast | 28 |
| Yufa | | Southeast | 29 |
| Liulihe | | Southwest | 30 |
| Qianmen East Street | Traffic Monitoring Sites (to evaluate the impact of road traffic pollution on ambient air quality) | Center | 31 |
| Yongdingmen Inner Street | | Center | 32 |
| Xizhimen North Street | | Center | 33 |
| South 3rd Ring Road | | Center | 34 |
| East 4th Ring Road | | Center | 35 |

In addition, the data of daily total radiation were obtained by the China Meteorological Data Sharing Service System Administration (available online: http://data.cma.cn/site/index.html) from December 2016 to February 2017.

### 2.3. Data Analysis

Daily (24-h) mean concentrations of $PM_{2.5}$ and $O_3$ concentrations were calculated in order to study the seasonal variations. We calculated the diurnal variations of $PM_{2.5}$ and $O_3$ concentrations during two seasons by averaging the concentrations at same time points of all days per season. The limit value for daily $PM_{2.5}$ concentration was defined as the new National Ambient Air Quality Standards (NAAQS-China, GB3095-2012) (75 $\mu g/m^3$). For $O_3$, we used the daily maximum 8-h $O_3$ concentration (160 $\mu g/m^3$) and the daily maximum 1-h $O_3$ concentration (200 $\mu g/m^3$) (Available online: http://www.mee.gov.cn/).

For spatial comparison, we calculated the average concentrations of $PM_{2.5}$ and $O_3$ in each region of Beijing according to the location of each site [42]. The regions of Beijing were defined based on geographical administrative divisions, as shown in Table 1.

We used Inverse Distance Weighted (IDW) to interpolate the air pollution data from the 35 monitoring stations to general spatial maps for spatial comparison. This method for spatial interpolation was applied to characterize spatial distributions of pollutant concentrations in some studies [43–46]. The IDW-based interpolation maps of $PM_{2.5}$ and $O_3$ were produced using a random 70% of points [15] and validated with the remaining 30% of data. In addition, the root mean square error of $PM_{2.5}$ and $O_3$ concentration maps were calculated as an indication of the accuracy of the interpolation maps. Spatial distribution maps of $PM_{2.5}$ and $O_3$ concentrations were produced using ArcGIS ArcMap 10.0 software (Available online: http://www.esri.com/).

In order to further study secondary formation of $PM_{2.5}$ under different $O_{3,max}$ in summer, CO is usually considered as a tracer of primary combustion source, and the $PM_{2.5}$/CO ratio is an indicator to qualitatively infer the contribution of secondary aerosols [47].

In order to analyze the correlation between $PM_{2.5}$ and $O_3$, the statistical analysis was performed using two-tailed test, which showed that these data did not obey normal distribution. Then, Pearson correlation coefficients were calculated in order to quantify the association between $PM_{2.5}$ and $O_3$. All *p*-values were two-tailed and $p < 0.05$ was considered statistically significant. All analyses were carried out using the Origin software (OriginLab 9.0, Origin Lab Corporation, Northampton, MA, USA).

## 3. Results

### *3.1. $PM_{2.5}$ and $O_3$ Concentrations*

As shown in Figure 2, the average $PM_{2.5}$ concentrations during the summer and winter were 58.02 μg/m$^3$ and 108.13 μg/m$^3$ respectively, with 29 days in summer and 46 days in winter exceeding the current NAAQS limit for $PM_{2.5}$. For $O_3$, the average concentration in summer was 91.26 μg/m$^3$ with 44 days exceeding the current NAAQS limit, and the average concentration in winter was 30.33 μg/m$^3$ with no days over the limit.

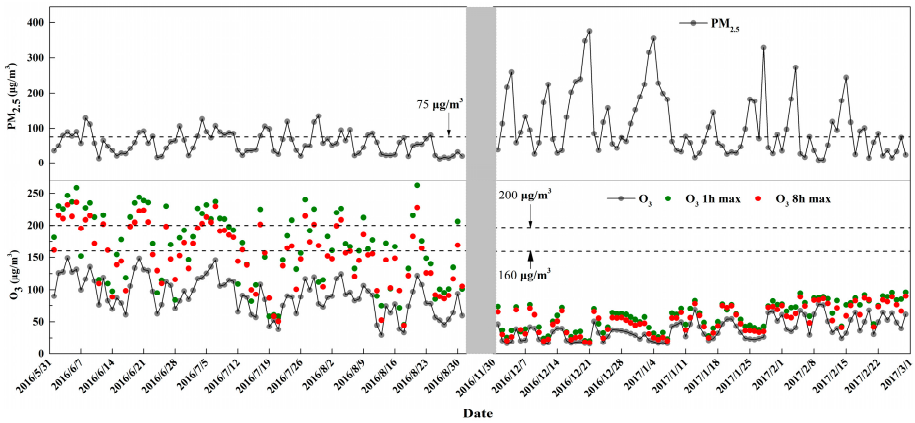


**Figure 2.** The daily average concentrations of $PM_{2.5}$ and $O_3$ in the two seasons in Beijing (the green dots indicate $O_3$ 1h max and the red dots indicate $O_3$ 8h max).

$PM_{2.5}$ presented the highest concentrations at traffic sites both in summer and in winter, followed by urban, suburban, and background sites (60.51, 54.28, and 54.94 μg/m$^3$ in summer and 105.51, 102.16, and 109.62 μg/m$^3$ in winter, respectively), as shown in Figure 3. On the contrary, $O_3$ concentrations were lowest at traffic monitoring sites and higher at background/suburban sites. Specifically, $O_3$ concentrations were 73.52 (24.04) μg/m$^3$ at traffic sites in the summer (winter), and reached 92.13 (29.76), 96.82 (34.02), and 94.31 (34.42) μg/m$^3$ at urban, suburban, and background sites, respectively.

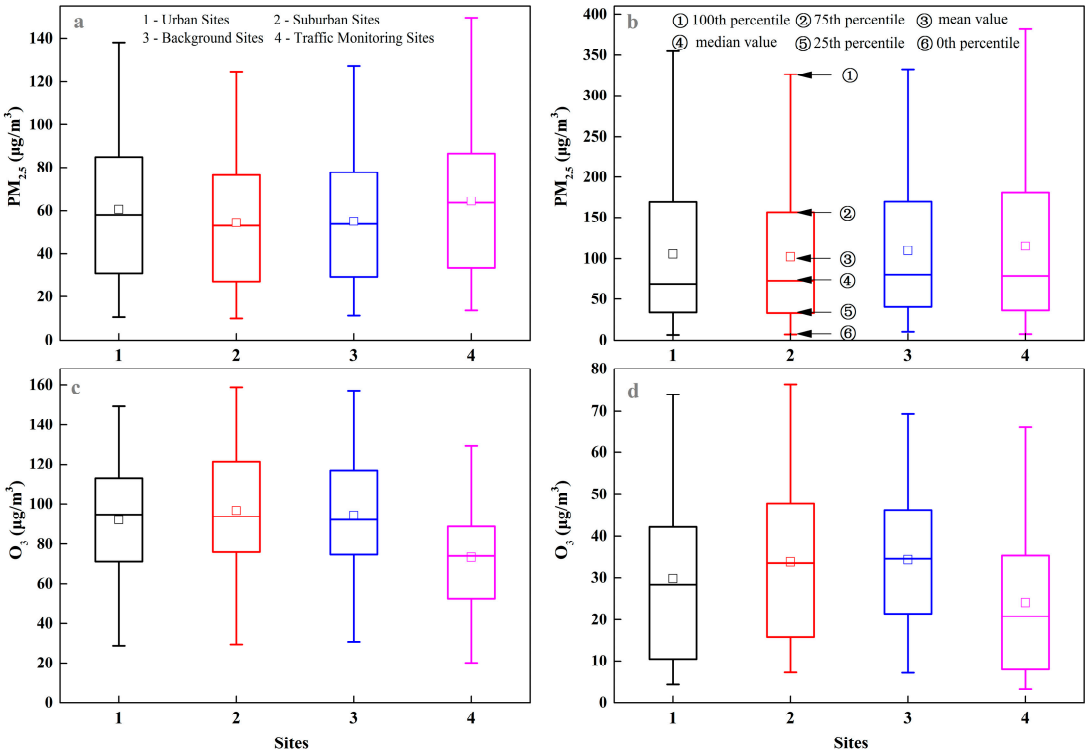


**Figure 3.** $PM_{2.5}$ and $O_3$ concentrations in different kinds of air monitoring sites ((**a**) $PM_{2.5}$ concentration during summer, (**b**) $PM_{2.5}$ concentration during winter, (**c**) $O_3$ concentration during summer, and (**d**) $O_3$ concentration during winter). The whiskers above and below the boxes indicate the 100th and 0th percentiles, the upper and lower boundaries of the boxes indicate the 75th and 25th percentiles, the squares indicate the mean values, and the lines in the boxes indicate the median values.

### *3.2. Diurnal Variations in $PM_{2.5}$ and $O_3$ Concentrations*

$PM_{2.5}$ and $O_3$ concentrations presented a distinct diurnal pattern over the seasons across sites (see Figure 4). During summer, $PM_{2.5}$ concentrations were higher in the daytime than in the nighttime, with the highest concentrations always recorded at traffic sites. In general, during summer, $PM_{2.5}$ concentrations began to rise early in the morning at around 4:00–5:00, reaching a peak around 8:00–9:00, successively decreasing until reaching the minimum at around 16:00–17:00, followed by a new rise until 21:00–23:00. Except for background sites, other sites showed similar characteristics, with two valley values at 4:00–5:00 and 16:00–17:00, and two peak values at 8:00–9:00 and 20:00–23:00, respectively; this is consistent with previous observations [48]. The highest $PM_{2.5}$ concentrations in urban, suburban, background, and traffic sites were 66.92 μg/m$^3$, 58.66 μg/m$^3$, 62.03 μg/m$^3$, and 70.68 μg/m$^3$, respectively. The lowest $PM_{2.5}$ concentration in suburban and background sites was ~50 μg/m$^3$, while it was approximately 55–60 μg/m$^3$ at the other two sites types. On the contrary, $PM_{2.5}$ concentrations presented the opposite pattern during winter, with lower concentrations in the daytime than in the nighttime. For suburban and background sites, $PM_{2.5}$ concentrations gradually reduced from 0:00–8:00, and then increased to a small peak at around 9:00–10:00; the lowest $PM_{2.5}$ concentrations appeared at 15:00. For urban and traffic sites, $PM_{2.5}$ concentrations began to decrease at 0:00–1:00 and reached the lowest level (85–95 μg/m$^3$) at 11:00, followed by a sharp increase to the maximum level (125–145 μg/m$^3$) around 23:00–1:00.

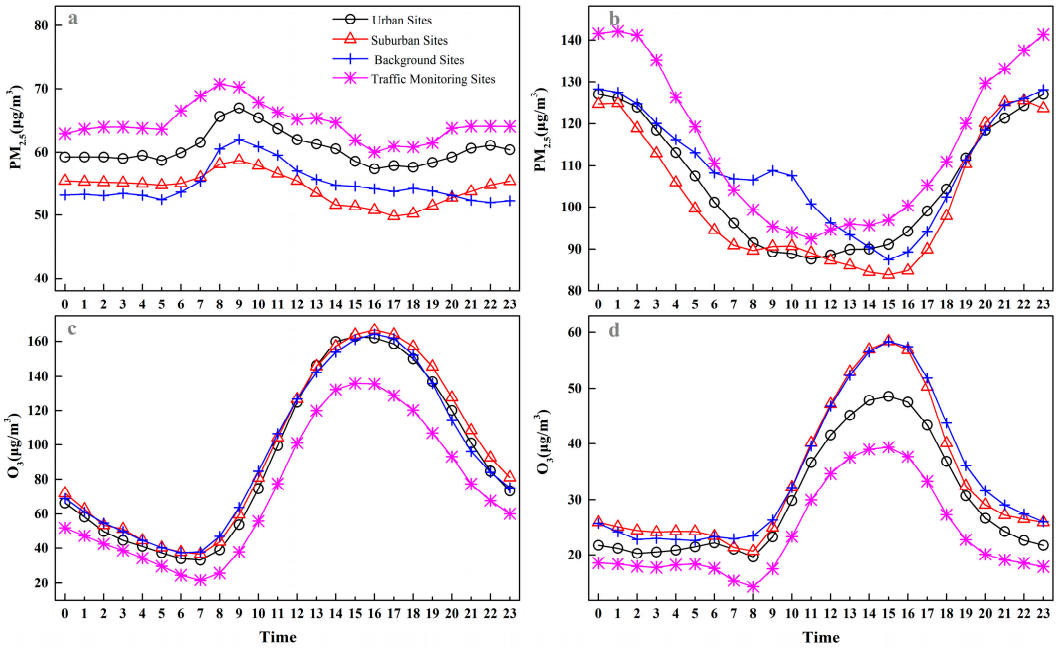


**Figure 4.** Average diurnal variations in $PM_{2.5}$ and $O_3$ concentrations: (**a**) $PM_{2.5}$ concentration during summer; (**b**) $PM_{2.5}$ concentration during winter; (**c**) $O_3$ concentration during summer; and (**d**) $O_3$ concentration during winter.

Although the $O_3$ concentrations showed a statistically significant difference ($p < 0.05$) between the two seasons, traffic monitoring sites always present lower $O_3$ concentrations than the other three site types. Interestingly, the four monitoring sites presented similar diurnal variation in the summer: the lowest $O_3$ concentrations were observed at 7:00 in the morning. The lowest value was less than 20 μg/m$^3$ in traffic monitoring sites, while values were between 30 and 40 μg/m$^3$ at the other three site types. $O_3$ concentrations for all four sites increased from 7:00 until around 15:00–16:00, when they reached their peak. The highest $O_3$ concentration in urban, suburban, and background sites was around 160–170 μg/m$^3$, while it was about 130 μg/m$^3$ at traffic sites. During the nighttime, $O_3$ concentrations exhibited a decrease. After midnight, they presented a relatively stable phase, in agreement with previous observations [49]. The pattern of the diurnal variations of $O_3$ in winter was similar to that in summer, although with reduced fluctuation. The minimum $O_3$ concentrations appeared at 08:00 (except for background sites) followed by an increase to the highest value at 15:00, and then a gradual decrease until the next morning.

### *3.3. Spatial Variations in $PM_{2.5}$ and $O_3$ Concentrations*

Figure 5 illustrates average concentrations of $PM_{2.5}$ and $O_3$ in each region. $PM_{2.5}$ concentration was significantly higher ($p < 0.01$) in winter than in summer, while $O_3$ concentration was significantly lower ($p < 0.01$) in winter than in summer. The highest $PM_{2.5}$ concentrations in the two seasons were observed in Southeast Beijing. $PM_{2.5}$ concentrations were much lower in northwest and northeast of Beijing than in the rest of the regions in the two seasons. Northwest and northeast presented the lowest $PM_{2.5}$ concentrations in summer and the highest $O_3$ concentrations in winter.

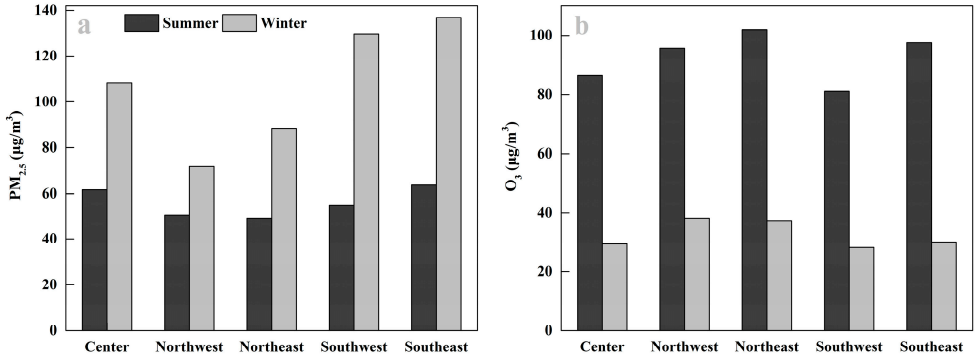


**Figure 5.** Average concentrations of $PM_{2.5}$ and $O_3$ in each region of Beijing. (**a**) Concentration of $PM_{2.5}$. (**b**) Concentration of $O_3$.

Figure 6 presents the $O_3$ and $PM_{2.5}$ spatial distribution in Beijing, obtained by inverse distance weighted algorithm; RMSEs of $PM_{2.5}$ and $O_3$ maps were equal to 3.01 (about 5.11%) and 10.03 (about 11.21%) μg/m$^3$ for summer and 12.93 (about 11.33%) and 5.59 μg/m$^3$ (about 16.76%) for winter, respectively.

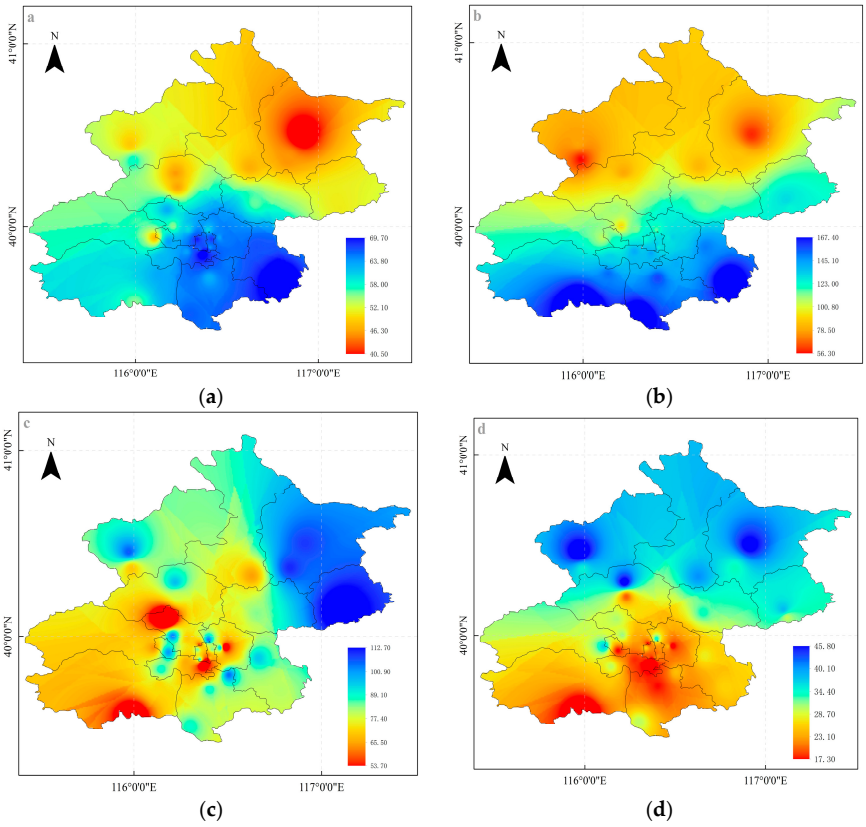


(**a**) (**b**) (**c**) (**d**)

**Figure 6.** Spatial distribution in $PM_{2.5}$ and $O_3$ concentrations in Beijing: (**a**) $PM_{2.5}$ concentration during summer; (**b**) $PM_{2.5}$ concentration during winter; (**c**) $O_3$ concentration during summer; and (**d**) $O_3$ concentration during winter.

Overall, $PM_{2.5}$ pollution was significantly higher in the southern part of Beijing than in the northern area ($p < 0.01$), and this pattern was especially obvious in winter. On the contrary, $O_3$ concentrations presented decreasing concentrations from north to south, especially during summer.

### *3.4. Interaction between $PM_{2.5}$ and $O_3$ during the Summer and Winter Seasons*

To better understand the interaction of $PM_{2.5}$ and $O_3$ in the atmosphere, we examined the correlations of daily mean $PM_{2.5}$ and $O_3$ concentrations (see Figure 7). The results indicated that $PM_{2.5}$ concentrations were positively correlated ($p < 0.01$, $r = 0.57$) with $O_3$ concentrations in summer, but negatively correlated ($p < 0.01$, $r = -0.72$) with $O_3$ concentrations in winter.

To study the effect of $O_3$ concentrations on $PM_{2.5}$ concentrations in summer, the diurnal variation of $PM_{2.5}$ was displayed under four $O_{3,max}$ (daily maximum $O_3$ concentration) levels (see Figure 8) [38]: exceeding 200 μg/m$^3$, from 160 to 200 μg/m$^3$, from 100 to 160 μg/m$^3$, and below 100 μg/m$^3$. When $O_{3,max}$ was greater than 200 μg/m$^3$, $PM_{2.5}$ concentration was the highest and the diurnal variation was significant, with the maximum $PM_{2.5}$ concentration observed at 10:00. When $O_{3,max}$ was between 160 and 200 μg/m$^3$, $PM_{2.5}$ concentration was relatively high and the maximum concentration was observed at 08:00. When $O_{3,max}$ was between 100 to 160 μg/m$^3$ and less than 100 μg/m$^3$, $PM_{2.5}$ concentrations were low with the maximum hourly concentrations occurring at 23:00 and 00:00, respectively. On the whole, $PM_{2.5}$ levels were higher when $O_3$ levels were higher in summer. In addition, we also averaged the $PM_{2.5}/CO$ ratio under different $O_{3,max}$ in summer, as shown in Figure 9. When $O_{3,max}$ exceeded 200 μg/m$^3$, 160–200 μg/m$^3$, 100–160 μg/m$^3$, and below 100 μg/m$^3$, respectively, the average $PM_{2.5}/CO$ ratios were 0.083, 0.075, 0.055, and 0.048, respectively.

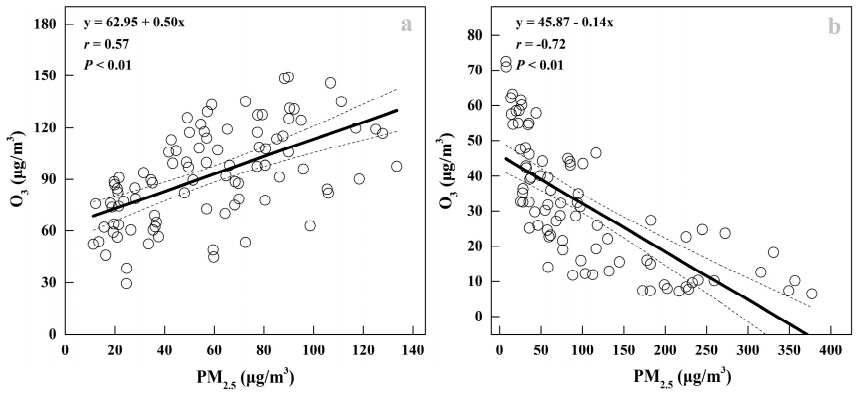


**Figure 7.** Scatter plots of $PM_{2.5}$ vs. $O_3$ during the summer and winter seasons (**a**) in summer and (**b**) in winter.

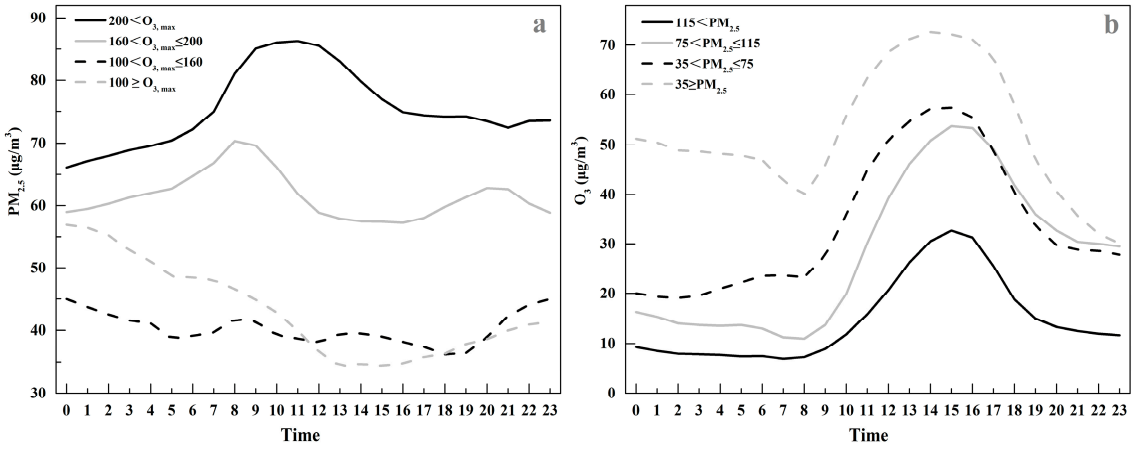


**Figure 8.** Diurnal variations in $PM_{2.5}$ and $O_3$ concentrations under different $O_{3,max}$ and $PM_{2.5}$ levels, respectively. (**a**) Diurnal variation of $PM_{2.5}$ under four $O_{3,max}$ levels: exceeding 200 μg/m$^3$, 160–200 μg/m$^3$, 100–160 μg/m$^3$, and below 100 μg/m$^3$ in summer. (**b**) Diurnal variation of $O_3$ under four $PM_{2.5}$ levels: exceeding 115 μg/m$^3$, 75–115 μg/m$^3$, 35–75 μg/m$^3$, and below 35 μg/m$^3$ in winter.

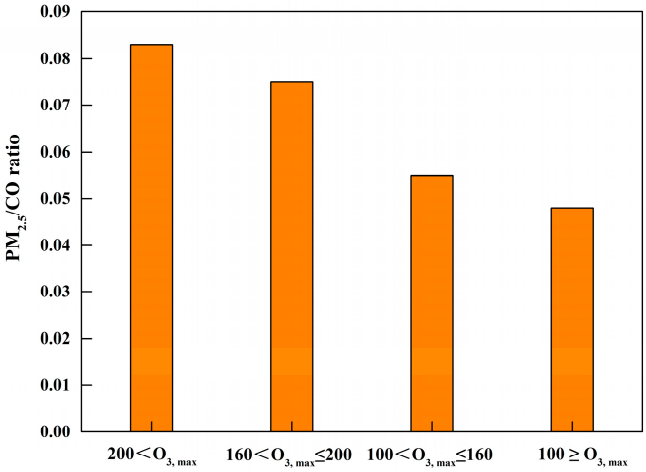


**Figure 9.** Average $PM_{2.5}$/CO ratio under different $O_{3,max}$ in summer.

To study the effect of $PM_{2.5}$ concentration on $O_3$ concentration in winter, we analyzed the diurnal variation of $O_3$ under four $PM_{2.5}$ levels, selected on the basis of previous researches by Jia et al. [38]: exceeding 115 μg/m$^3$, from 75 to 115 μg/m$^3$, from 35 to 75 μg/m$^3$, and below 35 μg/m$^3$. When $PM_{2.5}$ level was greater than 115 μg/m$^3$, $O_3$ concentration was low with small hourly variation. When $PM_{2.5}$ levels were between 75 to 115 μg/m$^3$ and between 35 to 75 μg/m$^3$, $O_3$ concentrations further increased, with the previously described hourly variations. When $PM_{2.5}$ level was less than 35 μg/m$^3$, $O_3$ concentration was the highest with large hourly variation. In general, $O_3$ levels were lower when $PM_{2.5}$ levels were higher in winter. We also averaged the daily total radiation under different $PM_{2.5}$ levels in winter, as shown in Figure 10. When $PM_{2.5}$ levels exceeded 115 μg/m$^3$, 75–115 μg/m$^3$, 35–75 μg/m$^3$, and below 35 μg/m$^3$, respectively, the average daily total radiation was 6.07 MJ/m$^2$, 9.24 MJ/m$^2$, 10.40 MJ/m$^2$, and 13.76 MJ/m$^2$, respectively.

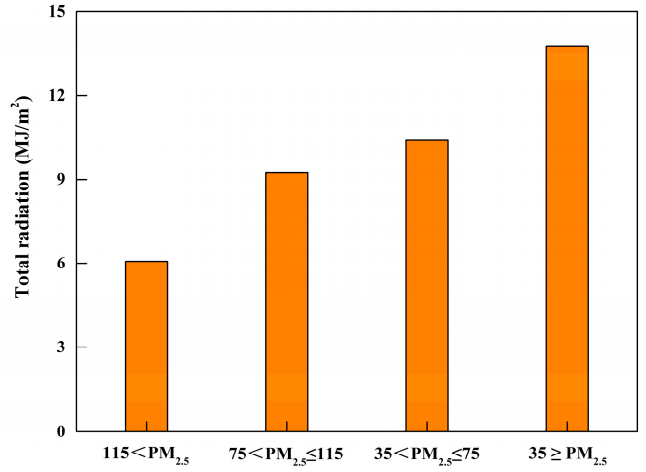


**Figure 10.** Average daily total radiation under different $PM_{2.5}$ levels in winter.

## 4. Discussion

Undoubtedly, in recent years, atmospheric compound pollution characterized by $PM_{2.5}$ and $O_3$ has caused negative effects on atmospheric visibility, human health, and climate change [50–52]. Particulate matter in the atmosphere can not only affect air quality and human health, but also affects the earth's radiation budget [53]. In addition, Feng et al. [54] showed that current $O_3$ concentrations across China were sufficiently high to affect the yield and quality of agricultural crops. In addition, $O_3$ can also make an impact on human health. Numerous epidemiological studies found that $O_3$ had an association with premature mortality [55]. A recent study reported that $O_3$ has replaced $PM_{2.5}$ as

the chief pollutant in economically developed areas of China (e.g., Beijing-Tianjin-Hebei, Yangtze River Delta, and Pearl River Delta) [56]. In China, the annual average concentrations of $O_3$ and $PM_{2.5}$ were 49.00 $\mu g/m^3$ and 63.70 $\mu g/m^3$ in 2014, whereas in 2015, concentrations of $O_3$ and $PM_{2.5}$ increased and decreased by 7.40% and 12.00%, respectively [57]. Therefore, studies on the evolution of $PM_{2.5}$ and $O_3$ and their relationships over time across space are essential for a better understanding and planning of policies for air pollution control.

In this study, we found that $PM_{2.5}$ concentrations in Beijing were lower in summer than in winter, while $O_3$ concentrations were higher in summer than in winter. Higher $PM_{2.5}$ concentrations were observed in winter, which is attributed to a large number of anthropogenic emissions from biomass burning and combustion of fossil fuels and unfavorable weather conditions (e.g., low temperature, weak solar radiation, and low boundary layer height) for the dilution and diffusion of $PM_{2.5}$ [8,34,58]. Meteorological factors and $O_3$ precursors are linked to $O_3$ formation [59–61]. Generally, higher temperatures and enhanced solar radiation can result in an elevated rate of photochemical reaction that promotes the production of ozone [7,62], which explains why $O_3$ concentration is higher in summer than in winter, as observed in this study. In addition, relative humidity is also an important factor determining $O_3$ levels. Enhanced relative humidity is favorable for aerosol formation [63], and high aerosol concentration can decrease photochemical activities and inhibit the formation of $O_3$ [64,65]. The higher $PM_{2.5}$ concentrations observed at traffic monitoring sites during both the winter and summer seasons are linked to their vicinity to traffic emission sources [48], which increases $PM_{2.5}$ pollution. However, the results also indicated that traffic monitoring sites had much lower $O_3$ concentrations than other sites. This is due to the high concentration of primary NO present at traffic sites, which favor $O_3$ titration, while at rural areas reduced NO concentrations together with higher VOCs emissions (biogenic) favor $O_3$ formation [32,66]. In particular, some studies showed that local $O_3$ production was controlled by the VOC/$NO_X$ ratio [67]. In this case, $O_3$ concentration increases with increasing VOC concentration, but decreases with increasing NOx concentration. Usually, urban sites show relatively low VOC/NOx ratios due to high $NO_X$ emission [68]. In addition, $O_3$ is also generated during the transport of its precursors from urban areas to suburban areas [69,70]. Overall, the higher VOC/NOx ratios and/or transport of $O_3$ and precursors from urban areas can explain the observation of higher $O_3$ levels at suburban sites than at urban sites [71].

The higher daytime $PM_{2.5}$ concentrations in summer can be explained by the stronger atmospheric oxidation favoring secondary aerosol production [72–74]. The forenoon peak of $PM_{2.5}$ concentrations is probably due to enhanced anthropogenic activity during rush hour [34], and the decreasing $PM_{2.5}$ concentrations after sunrise is mainly caused by the higher boundary layer height, which favors the dilution or diffusion of $PM_{2.5}$. The boundary layer height usually remains high for longer time in summer afternoons, leading to a plateau in $PM_{2.5}$ concentrations [75]. The early nighttime peak may result from a combination of the reduced boundary height and enhanced anthropogenic activity during rush hours [42]. Overall, the lower nighttime $PM_{2.5}$ concentrations in summer are likely associated with the reductions in source activities and removal of particles by dry deposition [76], a mechanism enhanced for hygroscopic particles by the increase in relative humidity. In winter, $PM_{2.5}$ concentrations were higher during nighttime than during daytime. The boundary layer height usually decreases early in the afternoon due to decreased solar radiation, resulting in low $PM_{2.5}$ concentrations during noontime [76]. Decreased boundary layer height and wind speed and increased source activity during the afternoon rush hour lead to higher $PM_{2.5}$ concentrations during evening hours [34,76]. However, the diurnal variations of $O_3$ concentrations during the two seasons were almost the same, with a single-peak occurring at 16:00 and 15:00 in summer and winter, respectively. During both seasons, $O_3$ concentration peaks result from higher solar radiation and temperatures promoting photochemical formation of $O_3$ [72].

Spatially, $PM_{2.5}$ concentrations in Southern Beijing were higher than in Northern Beijing during the two seasons, and this pattern was especially evident in winter. This can result from regional transport of $PM_{2.5}$ from neighboring heavily polluted cities of Southern Beijing (e.g., Tianjin, Langfang,

Baoding, and Zhangjiakou) [49,77,78], while Northern Beijing is surrounded by mountains. In addition, the lower population density with reduced human activity in Northern Beijing could contribute to lower $PM_{2.5}$ concentration [8]. Conversely, $O_3$ concentrations showed a decreasing trend from the north to the south during the two seasons; this pattern was more evident in summer. A previous study showed that AOD in Southern Beijing was higher than in Northern Beijing [79], suggesting that surface solar radiation was stronger in Northern Beijing than in Southern Beijing, which favored photochemical $O_3$ production. Further, higher biogenic VOCs emissions due to the presence of vegetation in Northern Beijing can favor $O_3$ formation [80]. On the other hand, the higher NOx concentrations observed in Southern Beijing favor $O_3$ titration [81,82].

A significant positive correlation in summer and a significant negative correlation in winter were observed between $PM_{2.5}$ and $O_3$. The formation mechanisms and sources of $PM_{2.5}$ are very complex. Recent studies have suggested that secondary aerosols might dominate the $PM_{2.5}$ mass [83]. We compared the $PM_{2.5}/CO$ ratio under different $O_{3,max}$ in summer, and found that the $PM_{2.5}/CO$ ratio increased with rising in $O_{3,max}$, reflecting the fact that the contribution of secondary aerosols increased with rising in $O_{3,max}$. Thus, the significant positive correlation between $PM_{2.5}$ and $O_3$ is likely due to the fact that high $O_3$ concentrations with strong atmospheric oxidation in summer can promote the enhanced photochemical formation of secondary fine particulates [35,38]. Additionally, we also compared the daily total radiation under different $PM_{2.5}$ levels in winter, and found that the daily total radiation decreased with rising in $PM_{2.5}$, suggesting that high $PM_{2.5}$ concentrations in winter could potentially weaken the intensity of solar radiation reaching the Earth's surface and inhibit the formation of $O_3$, leading to a negative relation between $PM_{2.5}$ and $O_3$.

## 5. Conclusions

In summary, we analyzed the spatiotemporal distribution characteristics in $PM_{2.5}$ and $O_3$ in Beijing and investigated their interaction mechanisms in summer and winter based on hourly $PM_{2.5}$ and $O_3$ data for all 35 sites. The results showed that $PM_{2.5}$ concentrations were significantly lower ($p < 0.05$) in summer than in winter, while $O_3$ concentrations were significantly higher ($p < 0.05$) in summer than in winter. Among sites, traffic monitoring sites showed the highest $PM_{2.5}$ concentration and the lowest $O_3$ concentration during the two seasons. A remarkably different diurnal variation of $PM_{2.5}$ concentration was observed between summer and winter ($p < 0.05$), with the higher concentration during daytime summer and nighttime winter. Diurnal variations in $O_3$ concentration during the two seasons were observed as a single peak at 16:00 and 15:00 in summer and winter, respectively. Spatially, $PM_{2.5}$ concentrations decreased in gradient from the south to the north. On the contrary, $O_3$ concentrations in Northern Beijing were higher than those in Southern Beijing.

Our findings also confirmed that high $O_3$ concentrations with strong atmospheric oxidation in summer could promote the enhanced photochemical formation of secondary fine particulates, and the enhanced $PM_{2.5}$ levels in winter could potentially suppressed the intensity of surface solar radiation and inhibit the formation of $O_3$.

According to the discussion and analysis of this study, we propose the following suggestions for future direction of air pollution control. First, although Beijing currently has 35 air quality monitoring stations, their spatial distribution is not uniform. As shown in Figure 1, most of the stations are sited in the urban areas of Beijing and thus more monitoring stations should be established in suburban areas. Second, previous studies have shown that air pollution in Beijing is strongly influenced by regional atmospheric pollutant transportation from the surrounding areas. Consequently, regional cooperation and joint defense and control are effective ways to control air pollution. Third, Beijing's government has implemented a series of air pollution control policies and regulations to improve air quality in recent years. These measures have favored the reduction of $PM_{2.5}$, but $O_3$ concentration showed an increasing trend. Thus, it is recommended that more studies be conducted on the pollution characteristics, sources, and formation processes of $O_3$. Finally, this study reveals the interaction between $PM_{2.5}$ and $O_3$, and

indicates that the coordinated control of $PM_{2.5}$ and $O_3$ is the future research direction in the field of atmospheric environment in Beijing.

In conclusion, the formation process and interaction of $PM_{2.5}$ and $O_3$ are very complex, as they are not only affected by primary emissions but also affected by other influencing factors including meteorological conditions, transformation of precursors, and atmospheric oxidant capacity, suggesting further investigation is needed.

**Author Contributions:** H.Z. and Y.Z. conceived and designed the experiments as well as wrote the paper; H.Z. analyzed the data; and C.L. helped perform the statistical analysis.

**Fund:** This research was funded by the National Natural Science Foundation of China (Grant No. 41475108), Postgraduate Research & Practice Innovation Program of Jiangsu Province (Grant No. KYCX17_0878), and the Visiting Fellowship from China Scholarship Council (Grant No. 201708320313).

**Conflicts of Interest:** The authors declare no conflicts of interest.

## References

1. Hu, J.L.; Wang, Y.G.; Ying, Q.; Zhang, H.L. Spatial and temporal variability of $PM_{2.5}$ and $PM_{10}$ over the North China Plain and the Yangtze River Delta, China. *Atmos. Environ.* **2014**, *95*, 598–609. [CrossRef]
2. Torretta, V.; Rada, E.C.; Capodaglio, A.G. An example of the use of bio-indicators for air quality assessment in areas with high industrial presence. *Environ. Eng. Manag. J.* **2015**, *14*, 2679–2687.
3. Mannucci, P.M.; Franchini, M. Health effects of ambient air pollution in developing countries. *Int. J. Environ. Res. Public Health* **2017**, *14*, 1048. [CrossRef] [PubMed]
4. Aranda, A.; Mera, Y.D.; Notario, A.; Rodriguez, D.; Rodriguez, A. Fine and ultrafine particles in small cities. A case study in the south of Europe. *Environ. Sci. Pollut. Res.* **2015**, *22*, 18477–18486. [CrossRef] [PubMed]
5. Debaje, S.B. Estimated crop yield losses due to surface ozone exposure and economic damage in India. *Environ. Sci. Pollut. Res.* **2014**, *21*, 7329–7338. [CrossRef] [PubMed]
6. Zhang, Z.Y.; Zhang, X.L.; Gong, D.Y.; Quan, W.J.; Zhao, X.J.; Ma, Z.Q.; Kim, S.J. Evolution of surface $O_3$ and $PM_{2.5}$ concentrations and their relationships with meteorological conditions over the last decade in Beijing. *Atmos. Environ.* **2015**, *108*, 67–75. [CrossRef]
7. Guo, H.; Wang, Y.G.; Zhang, H.L. Characterization of criteria air pollutants in Beijing during 2014–2015. *Environ. Res.* **2017**, *154*, 334–344. [CrossRef] [PubMed]
8. Guo, S.; Hu, M.; Zamora, M.L.; Peng, J.F.; Shang, D.J.; Zheng, J.; Du, Z.F.; Wu, Z.J.; Shao, M.; Zeng, L.M.; et al. Elucidating severe urban haze formation in China. *Proc. Natl. Acad. Sci. USA* **2014**, *111*, 17373–17378. [CrossRef] [PubMed]
9. Mills, G.; Hayes, F.; Simpson, D.; Emberson, L.; Norris, D.; Harmens, H.; Buker, P. Evidence of widespread effects of ozone on crops and (semi-) natural vegetation in Europe (1990–2006) in relation to AOT40- and flux-based risk maps. *Global. Change Biol.* **2011**, *17*, 592–613. [CrossRef]
10. Sicard, P.; Anav, A.; Marco, A.D.; Paoletti, E. Projected global tropospheric ozone impacts on vegetation under different emission and climate scenarios. *Atmos. Chem. Phys.* **2017**, *17*, 12177–12196. [CrossRef]
11. Calatayud, V.; Diéguez, J.J.; Sicard, P.; Schaub, M.; Marco, A.D. Testing approaches for calculating stomatal ozone fluxes from passive samplers. *Sci. Total. Environ.* **2016**, *572*, 56–67. [CrossRef] [PubMed]
12. *State Environmental Protection Administration of China, State Bureau of Technical Supervision*; Ambient Air Quality Standard (GB3095–1996); China Standards Press: Beijing, China, 1996.
13. Chen, W.; Tang, H.Z.; Zhao, H.M. Urban air quality evaluations under two versions of the national ambient air quality standards of China. *Atmos. Pollut. Res.* **2016**, *7*, 49–57. [CrossRef]
14. Pausata, F.S.R.; Gaetani, M.; Messori, G.; Kloster, S.; Dentener, F.J. The role of aerosol in altering North Atlantic atmospheric circulation in winter and its impact on air quality. *Atmos. Chem. Phys.* **2015**, *15*, 1725–1743. [CrossRef]
15. Zhao, H.; Zheng, Y.F.; Li, T.; Wei, L.; Guan, Q. Temporal and spatial variation in, and population exposure to, summertime ground-level ozone in Beijing. *Int. J. Environ. Res. Public Health* **2018**, *15*, 628. [CrossRef] [PubMed]
16. Sikder, H.A.; Suthawaree, J.; Kato, S.; Kajii, Y. Surface ozone and carbon monoxide levels observed at Oki, Japan: Regional air pollution trends in East Asia. *J. Environ. Manag.* **2011**, *92*, 953–959. [CrossRef] [PubMed]

17. Jeon, W.B.; Lee, S.H.; Lee, H.; Park, C.; Kim, D.H.; Park, S.Y. A study on high ozone formation mechanism associated with change of NOx/VOCs ratio at a rural area in the Korean Peninsula. *Atmos. Environ.* **2014**, *89*, 10–21. [CrossRef]
18. Tong, N.Y.O.; Leung, D.Y.C.; Liu, C.H. A review on ozone evolution and its relationship with boundary layer characteristics in urban environments. *Water. Air. Soil Pollut.* **2011**, *214*, 13–36. [CrossRef]
19. Schiavon, M.; Torretta, V.; Casazza, A.; Ragazzi, M. Non-thermal plasma as an innovative option for the abatement of volatile organic compounds: A review. *Water. Air. Soil Pollut.* **2017**, *228*, 388. [CrossRef]
20. Schiavon, M.; Schiorlin, M.; Torretta, V.; Ragazzi, M.; Rada, E.C. Biofiltration combined with non-thermal plasma for air pollution control: A preliminary investigation. *Int. J. Sustain. Dev. Plan.* **2016**, *4*, 627–635. [CrossRef]
21. Collet, S.; Kidokoro, T.; Karamchandani, P.; Shah, T. Future-year ozone isopleths for South Coast, San Joaquin Valley, and Maryland. *Atmosphere* **2018**, *9*, 354. [CrossRef]
22. Thompson, D.R.; Kahn, B.H.; Green, R.O.; Chien, S.A.; Middleton, E.M.; Tran, D.Q. Global spectroscopic survey of cloud thermodynamic phase at high spatial resolution, 2005–2015. *Atmos. Meas. Tech.* **2018**, *11*, 1019–1030. [CrossRef]
23. Guo, F.; Ju, Y.; Wang, G.; Alvarado, E.C.; Yang, X.; Ma, Y.; Liu, A. Inorganic chemical composition of $PM_{2.5}$ emissions from the combustion of six main tree species in subtropical china. *Atmos. Environ.* **2018**, *189*, 107–115. [CrossRef]
24. Schiavon, M.; Ragazzi, M.; Rada, E.C.; Torretta, V. Air pollution control through biotrickling filters: A review considering operational aspects and expected performance. *Crit. Rev. Biotechnol.* **2016**, *36*, 1143–1155. [CrossRef] [PubMed]
25. Hartono, D.; Lioe, B.; Zhang, Y.; Li, B.; Yu, J. Impacts of particulate matter ($PM_{2.5}$) on the behavior of freshwater snail Parafossarulus striatulus. *Sci. Rep.* **2017**, *7*, 644. [CrossRef] [PubMed]
26. Torretta, V.; Raboni, M.; Copelli, S.; Rada, E.C.; Ragazzi, M.; Ionescu, G.; Apostol, T.; Badea, A. Application of strategies for particulate matter reduction in urban areas: An Italian case. *UPB. Sci. Bull. Ser. D* **2013**, *75*, 1454–2358.
27. Qiu, X.; Duan, L.; Gao, J.; Wang, S.; Chai, F.; Hu, J.; Zhang, J.; Yun, Y. Chemical composition and source apportionment of $PM_{10}$ and $PM_{2.5}$ in different functional areas of Lanzhou, China. *J. Environ. Sci* **2016**, *40*, 75–83. [CrossRef] [PubMed]
28. Cai, S.Y.; Wang, Y.J.; Zhao, B.; Wang, S.X.; Chang, X.; Hao, J.M. The impact of the "Air Pollution Prevention and Control Action Plan" on $PM_{2.5}$ concentrations in Jing-Jin-Ji region during 2012–2020. *Sci. Total. Environ.* **2017**, *580*, 197–209. [CrossRef] [PubMed]
29. Liu, H.; Wang, X.M.; Pang, J.M.; He, K.B. Feasibility and difficulties of China's new air quality standard compliance: PRD case of $PM_{2.5}$ and ozone from 2010 to 2025. *Atmos. Chem. Phys.* **2013**, *13*, 12013–12027. [CrossRef]
30. Sicard, P.; Serra, R.; Rossello, P. Spatiotemporal trends in ground-level ozone concentrations and metrics in France over the time period 1999–2012. *Environ. Res.* **2016**, *149*, 122–144. [CrossRef] [PubMed]
31. Kang, D.; Aneja, V.P.; Mathur, R.; Ray, J.D. Observed and modeled VOC chemistry under high VOC/NOx conditions in the Southeast United States national parks. *Atmos. Environ.* **2004**, *38*, 4969–4974. [CrossRef]
32. Wang, Z.S.; Li, Y.T.; Chen, T.; Li, L.J.; Liu, B.X.; Zhang, D.W.; Sun, F.; Wei, Q.; Jiang, L.; Pan, L.B. Changes in atmospheric composition during the 2014 APEC conference in Beijing. *J. Geophys. Res. Atmos.* **2015**, *120*, 12695–12707. [CrossRef]
33. Zhao, H.; Zheng, Y.F.; Wei, L.; Guan, Q.; Wang, Z.S. Evolution and evaluation of air quality in Hangzhou and its surrounding area during the G20 summit [in Chinese]. *China. Environ. Sci.* **2017**, *37*, 2016–2024.
34. Zhang, Y.L.; Cao, F. Fine particulate matter ($PM_{2.5}$) in China at a city level. *Sci. Rep.* **2015**, *5*, 14884. [CrossRef] [PubMed]
35. Chang, S.C.; Lee, C.T. Secondary aerosol formation through photochemical reactions estimated by using air quality monitoring data in Taipei City from 1994 to 2003. *Atmos. Environ.* **2007**, *41*, 4002–4017. [CrossRef]
36. Penn, S.L.; Arunachalam, S.; Woody, M.; Heiger-Bernays, W.; Tripodis, Y.; Levy, J.I. Estimating state-specific contributions to $PM_{2.5}$ and $O_3$ related health burden from residential combustion and electricity generating unit emissions in the United States. *Environ. Health. Persp.* **2017**, *125*, 324–332. [CrossRef] [PubMed]

37. Feng, T.; Bei, N.F.; Huang, R.J.; Cao, J.J.; Zhang, Q.; Zhou, W.J.; Tie, X.X.; Liu, S.X.; Zhang, T.; Su, X.L.; et al. Summertime ozone formation in Xi'an and surrounding areas, China. *Atmos. Chem. Phys.* **2016**, *15*, 4323–4342. [CrossRef]
38. Jia, M.W.; Zhao, T.L.; Cheng, X.H.; Gong, S.L.; Zhang, X.Z.; Tang, L.L.; Liu, D.Y.; Wu, X.H.; Wang, L.M.; Chen, Y.S. Inverse relations of $PM_{2.5}$ and $O_3$ in air compound pollution between cold and hot seasons over an urban area of east China. *Atmosphere* **2017**, *8*, 59. [CrossRef]
39. Xiao, Z.M.; Zhang, Y.F.; Hong, S.M.; Bi, X.H.; Jiao, L.; Feng, Y.C.; Wang, Y.Q. Estimation of the main factors influencing haze, based on a long-term monitoring campaign in Hangzhou, China. *Aerosol. Air. Qual. Res.* **2011**, *11*, 873–882. [CrossRef]
40. Song, S.J.; Wu, Y.; Xu, J.Y.; Ohara, T.; Hasegawa, S.C.; Li, J.Q.; Hao, J.M. Black carbon at a roadside site in Beijing: Temporal variations and relationships with carbon monoxide and particle number size distribution. *Atmos. Environ.* **2013**, *77*, 213–221. [CrossRef]
41. Li, R.K.; Li, Z.P.; Gao, W.J.; Ding, W.J.; Xu, Q.; Song, X.F. Diurnal, seasonal, and spatial variation of $PM_{2.5}$ in Beijing. *Sci. Bull.* **2015**, *60*, 387–395. [CrossRef]
42. Huang, F.F.; Li, X.; Wang, C.; Xu, Q.; Wang, W.; Luo, Y.X.; Tao, L.X.; Gao, Q.; Guo, J.; Chen, S.P.; et al. $PM_{2.5}$ spatiotemporal variations and the relationship with meteorological factors during 2013–2014 in Beijing, China. *PLoS ONE* **2015**, *10*, e0141642. [CrossRef] [PubMed]
43. Michanowicz, D.R.; Shmool, J.L.C.; Tunno, B.J.; Tripathy, S.; Gillooly, S.; Kinnee, E.; Clougherty, J.E. A hybrid land use regression/AERMOD model for predicting intra-urban variation in $PM_{2.5}$. *Atmos. Environ.* **2016**, *131*, 307–315. [CrossRef]
44. Lavi, A.; Potchter, O.; Omer, I.; Fireman, E. Mapping air pollution by biological monitoring in the metropolitan Tel Aviv area. *Int. J. Environ. Heal. Res.* **2015**, *26*, 346–360. [CrossRef] [PubMed]
45. Allshouse, W.B.; Adgate, J.L.; Blair, B.D.; McKenzie, L.M. A spatiotemporal industrial activity model for estimating the intensity of oil and gas operations in Colorado. *Environ. Sci. Technol.* **2017**, *51*, 10243–10250. [CrossRef] [PubMed]
46. Li, T.X.; Zhou, X.K.; Ikhumhen, H.O.; Difei, A. Research on the optimization of air quality monitoring station layout based on spatial grid statistical analysis method. *Environ. Technol.* **2017**, *39*, 1271–1283. [CrossRef] [PubMed]
47. Huang, R.J.; Zhang, Y.L.; Bozzetti, C.; Ho, K.F.; Cao, J.J.; Han, Y.M.; Daellenbach, K.R.; Slowik, J.G.; Platt, S.M.; Canonaco, F.; et al. High secondary aerosol contribution to particulate pollution during haze events in China. *Nature* **2014**, *514*, 218–222. [CrossRef] [PubMed]
48. Chen, W.; Tang, H.Z.; Zhao, H.M. Diurnal, weekly and monthly spatial variations of air pollutants and air quality of Beijing. *Atmos. Environ.* **2015**, *119*, 21–34. [CrossRef]
49. Cheng, L.J.; Wang, S.; Gong, Z.Y.; Li, H.; Yang, Q.; Wang, Y.Y. Regionalization based on spatial and seasonal variation in ground-level ozone concentrations across China. *J. Environ. Sci.* **2018**, *67*, 179–190. [CrossRef] [PubMed]
50. Shen, Y.L.; Yao, L. $PM_{2.5}$, Population exposure and economic effects in urban agglomerations of China using ground-based monitoring data. *Int. J. Environ. Res. Public Health* **2017**, *14*, 716. [CrossRef] [PubMed]
51. Wang, Y.Y.; Du, H.Y.; Xu, Y.Q.; Lu, D.B.; Wang, X.Y.; Guo, Z.Y. Temporal and spatial variation relationship and influence factors on surface urban heat island and ozone pollution in the Yangtze River Delta, China. *Sci. Total Environ.* **2018**, *631–632*, 921–933. [CrossRef] [PubMed]
52. Zheng, S.; Pozzer, A.; Cao, C.X.; Lelieveld, J. Long-term (2001–2012) concentrations of fine particulate matter ($PM_{2.5}$) and the impact on human health in Beijing, China. *Atmos. Chem. Phys.* **2015**, *15*, 5715–5725. [CrossRef]
53. Haywood, J.; Boucher, O. Estimates of the direct and indirect radiative forcing due to tropospheric aerosols: A review. *Rev. Geophys.* **2000**, *38*, 513–543. [CrossRef]
54. Feng, Z.Z.; Hu, E.Z.; Wang, X.k.; Jiang, L.J.; Liu, X.J. Ground-level $O_3$ pollution and its impacts on food crops in China: A review. *Environ. Pollut.* **2015**, *199*, 42–48. [CrossRef] [PubMed]
55. Wang, T.; Xue, L.; Brimblecombe, P.; Lam, Y.F.; Li, L.; Zhang, L. Ozone pollution in China: A review of concentrations, meteorological influences, chemical precursors, and effects. *Sci. Total Environ.* **2017**, *575*, 1582–1596. [CrossRef] [PubMed]
56. Liu, H.; Liu, S.; Xue, B.R.; Lv, Z.F.; Meng, Z.H.; Yang, X.F.; Xue, T.; Yu, Q.; He, K.B. Ground-level ozone pollution and its health impacts in China. *Atmos. Environ.* **2018**, *173*, 223–230. [CrossRef]

57. He, J.J.; Gong, S.L.; Yu, Y.; Yu, L.J.; Wu, L.; Mao, H.J.; Song, C.B.; Zhao, S.P.; Liu, H.L.; Li, X.Y.; et al. Air pollution characteristics and their relation to meteorological conditions during 2014–2015 in major Chinese cities. *Environ. Pollut.* **2017**, *223*, 484–496. [CrossRef] [PubMed]
58. Berkemeier, T.; Ammann, M.; Mentel, T.F.; Poschl, U.; Shiraiwa, M. Organic nitrate contribution to new particle formation and growth in secondary organic aerosols from α-pinene ozonolysis. *Environ. Sci. Technol.* **2016**, *50*, 6334–6342. [CrossRef] [PubMed]
59. Trieu, T.T.N.; Goto, D.; Yashiro, H.; Murata, R.; Sudo, K.; Tomita, H.; Satoh, M.; Nakajima, T. Evaluation of summertime surface ozone in Kanto area of Japan using a semi-regional model and observation. *Atmos. Environ.* **2017**, *153*, 163–181. [CrossRef]
60. Latif, M.T.; Huey, L.S.; Juneng, L. Variations of surface ozone concentration across the Klang Valley, Malaysia. *Atmos. Environ.* **2012**, *61*, 434–445. [CrossRef]
61. Pu, X.; Wang, T.J.; Huang, X.; Melas, D.; Zanis, P.; Papanastasiou, D.K.; Poupkou, A. Enhanced surface ozone during the heat wave of 2013 in Yangtze River Delta region, China. *Sci. Total Environ.* **2017**, *603–604*, 807–816. [CrossRef] [PubMed]
62. Rappengluck, B.; Perna, R.; Zhong, S.Y.; Morris, G.A. An analysis of the vertical structure of the atmosphere and the upper-level meteorology and their impact on surface ozone levels in Houston, Texas. *J. Geophys. Res. Atmos.* **2008**, *113*, D17315. [CrossRef]
63. Sun, Y.L.; Wang, Z.F.; Fu, P.Q.; Jiang, Q.; Yang, T.; Li, J.; Ge, X.L. The impact of relative humidity on aerosol composition and evolution processes during wintertime in Beijing, China. *Atmos. Environ.* **2013**, *77*, 927–934. [CrossRef]
64. Bian, H.; Han, S.Q.; Tie, X.X.; Sun, M.L.; Liu, A.X. Evidence of impact of aerosols on surface ozone concentration in Tianjin, China. *Atmos. Environ.* **2007**, *41*, 4672–4681. [CrossRef]
65. Yang, X.; Zhao, C.F.; Zhou, L.J.; Wang, Y.; Liu, X.H. Distinct impact of different types of aerosols on surface solar radiation in China. *J. Geophys. Res. Atmos.* **2016**, *121*, 6459–6471. [CrossRef]
66. Kulkarni, P.S.; Bortoli, D.; Silva, A.M. Nocturnal surface ozone enhancement and trend over urban and suburban sites in Portugal. *Atmos. Environ.* **2013**, *71*, 251–259. [CrossRef]
67. Pusede, S.E.; Cohen, R.C. On the observed response of ozone to NOx and VOC reactivity reductions in San Joaquin Valley California 1995-present. *Atmos. Chem. Phys.* **2012**, *12*, 9771–9811. [CrossRef]
68. Susaya, J.; Kim, K.H.; Shon, Z.H.; Brown, R.J.C. Demonstration of long-term increases in tropospheric $O_3$ levels: Causes and potential impacts. *Chemosphere* **2013**, *92*, 1520–1528. [CrossRef] [PubMed]
69. Sicard, P.; Marco, A.D.; Troussier, F.; Renou, C.; Vas, N.; Paoletti, E. Decrease in surface ozone concentrations at Mediterranean remote sites and increase in the cities. *Atmos. Environ.* **2013**, *79*, 705–715. [CrossRef]
70. Guerreiro, C.B.B.; Foltescu, V.; Leeuw, F.D. Air quality status and trends in Europe. *Atmos. Environ.* **2014**, *98*, 376–384. [CrossRef]
71. Paoletti, E.; Marco, A.D.; Beddows, D.C.S.; Harrison, R.M.; Manning, W.J. Ozone levels in European and USA cities are increasing more than at rural sites, while peak values are decreasing. *Environ. Pollut.* **2014**, *192*, 295–299. [CrossRef] [PubMed]
72. Wang, Z.S.; Li, Y.T.; Chen, T.; Zhang, D.W.; Sun, F.; Wei, Q.; Dong, X.; Sun, R.W.; Huan, N.; Pan, L.B. Ground-level ozone in urban Beijing over a 1-year period: Temporal variations and relationship to atmospheric oxidation. *Atmos. Res.* **2015**, *164–165*, 110–117. [CrossRef]
73. Murphy, S.M.; Sorooshian, A.; Kroll, J.H.; Ng, N.L.; Chhabra, P.; Tong, C.; Surratt, J.D.; Knipping, E.; Flagan, R.C.; Seinfeld, J.H. Secondary aerosol formation from atmospheric reactions of aliphatic amines. *Atmos. Chem. Phys.* **2007**, *7*, 2313–2337. [CrossRef]
74. Wen, L.; Chen, J.M.; Yang, L.X.; Wang, X.F.; Xu, C.H.; Sui, X.; Yao, Y.; Zhu, Y.H.; Zhang, J.M.; Zhu, T.; et al. Enhanced formation of fine particulate nitrate at a rural site on the North China Plain in summer: The important roles of ammonia and ozone. *Atmos. Environ.* **2015**, *101*, 294–302. [CrossRef]
75. Liu, Z.R.; Hu, B.; Wang, L.L.; Wu, F.K.; Gao, W.K.; Wang, Y.S. Seasonal and diurnal variation in particulate matter ($PM_{10}$ and $PM_{2.5}$) at an urban site of Beijing: Analyses from a 9-year study. *Environ. Sci. Pollut. Res.* **2015**, *22*, 627–642. [CrossRef] [PubMed]
76. Zhao, X.J.; Zhang, X.L.; Xu, X.F.; Xu, J.; Meng, W.; Pu, W.W. Seasonal and diurnal variations of ambient $PM_{2.5}$ concentration in urban and rural environments in Beijing. *Atmos. Environ.* **2009**, *43*, 2893–2900. [CrossRef]

77. Wang, D.F.; Zhou, B.; Fu, Q.Y.; Zhao, Q.B.; Zhang, Q.; Chen, J.M.; Yang, X.; Duan, Y.S.; Li, J. Intense secondary aerosol formation due to strong atmospheric photochemical reactions in summer: Observations at a rural site in eastern Yangtze River Delta of China. *Sci. Total. Environ.* **2016**, *571*, 1454–1466. [CrossRef] [PubMed]
78. Chai, F.H.; Gao, J.; Chen, Z.X.; Wang, S.L.; Zhang, Y.C.; Zhang, J.Q.; Zhang, H.F.; Yun, Y.R.; Ren, C. Spatial and temporal variation of particulate matter and gaseous pollutants in 26 cities in China. *J. Environ. Sci.* **2014**, *26*, 75–82. [CrossRef]
79. Fu, D.S.; Xia, X.A.; Wang, J.; Zhang, X.L.; Li, X.J.; Liu, J.Z. Synergy of AERONET and MODIS AOD products in the estimation of $PM_{2.5}$ concentrations in Beijing. *Sci. Rep.* **2018**, *8*, 10174. [CrossRef] [PubMed]
80. Li, G.; Bei, N.; Tie, X.; Molina, L.T. Aerosol effects on the photochemistry in Mexico City during MCMA-2006/MILAGRO campaign. *Atmos. Chem. Phys.* **2011**, *11*, 5169–5182. [CrossRef]
81. Sicard, P.; Dalstein-Richier, L.; Vas, N. Annual and seasonal trends of ambient ozone concentration and its impact on forest vegetation in Mercantour National Park (South-eastern France) over the 2000–2008 period. *Environ. Pollut.* **2011**, *159*, 351–362. [CrossRef] [PubMed]
82. Zhang, R.; Cohan, A.; Biazar, A.P.; Cohan, D.S. Source apportionment of biogenic contributions to ozone formation over the United States. *Atmos. Environ.* **2017**, *164*, 8–19. [CrossRef]
83. Cheng, N.L.; Zhang, D.W.; Li, Y.T.; Xie, X.M.; Chen, Z.Y.; Meng, F.; Gao, B.B.; He, B. Spatio-temporal variations of $PM_{2.5}$ concentrations and the evaluation of emission reduction measures during two red air pollution alerts in Beijing. *Sci. Rep.* **2017**, *7*, 8220. [CrossRef] [PubMed]